COHERENCE AND THE LOOK NUMBER—BASED DEFORMATION GRADIENT FUNCTION MODEL OF INSAR

M. Jiang [1], X. L. Ding [2] and Z. W. Li [3]
[1] Department of Land Surveying and Geo-Informatics,
The Hong Kong Polytechnic University, China. Email: 09901979r@polyu.edu.hk
[2] Department of Land Surveying and Geo-Informatics,
The Hong Kong Polytechnic University, China.
[3] School of Info-Physics and Geomatics Engineering,
Central South University, China.

ABSTRACT

A new functional model for determining the minimum and maximum detectable deformation gradients of the interferometric synthetic aperture radar (InSAR) is developed. The model incorporates both the interferometric coherence and the look number, representing an extension to the existing models that consider only the interferometric coherence. Experimental results with Envisat ASAR data show that the new model performs well for interferograms with different look numbers. The model can serve as an important tool in determining whether InSAR technology can be used effectively to monitor a particular given ground subsidence. In addition, the model can also be used to determine the optimum look number for multi-looking operation to result in the best deformation monitoring results.

KEYWORDS

InSAR, detectable deformation gradient (DDG), coherence, look number.

INTRODUCTION

Interferometric synthetic aperture radar (InSAR) has been widely used for ground deformation monitoring (Ding *et al.* 2004). However, it is not always possible to use InSAR to measure the deformations due to the various limitations of the technology (Wang *et al.* 2010; Li *et al.* 2007). It is therefore important to know when InSAR technology can be effectively used for deformation measurement and when it cannot. Such knowledge is essential in deciding wether the technology should be used and perhaps more importantly in avoiding mis-interpreting the results. For this purpose, detectable deformation gradient model (DDG), related the deformation gradient and the correlation between two radar echoes, was presented by Baran (Baran *et al.* 2005). In contrast with the previous study (Massonnet and Feigl 1998), since coherence is reflective for physical properties of the scatters and also a measure of interferometric noise, coherence-based DDG model can be applied in practice. However, phase noise in an interferogram is a function of both coherence and look number (Bamler and Hartl 1998). Moreover, multi-looking operation increases the size of the pixel, and also gives rise to phase aliasing when phase slopes are steep, which will significantly alter the minimum and maximum DDG.

In this study a new functional model for determining the minimum and maximum DDG by incorporating both the interferometric coherence and the look number is developed. The basic idea is to construct the first-order polynomial related DDG to coherence under each look number through statistics analysis of simulated observations and then generalize all linear polynomials to a function of two variables with linear least squares fitting. Different from pervious studies, semiautomatic fringe survey method has been employed to assist visual inspection for determining detectability of observations. On the other hand, the constraint defined on noise-free condition has been carefully modified. The model parameter such as coherence has also been corrected through an unbiased estimation algorithm.

OBSERVATIONS ESTABLISHMENT

The method presented in Baran *et al.*'s (2005) is slightly modified to establish observations: 1) select coherence values on real interferogram; 2) simulate deformation and calculate corresponding phase values; 3) introduce

phase into real SAR image; 4) interferometric process on modified pairs; 5) repeat steps 4) with the look numbers from 1 to 20. The details are shown below.

SAR data and Test site

Since the range and estimate accuracy of coherence values impact on polynomial coefficients of model during numerical statistics and regressions, the selection of study area and data set should be based on surface characteristics and sensor parameters on which the radar echoes correlation strongly relies. Therefore, the coherence observations employed in this paper are obtained with ENVISAT ASAR pair acquired in Feb. and Mar. 2005. The normal baseline is 215 m. The test site is located in Shanghai city, Yangtze River delta, China. The test site contains diverse land-cover: agriculture field, water body, forest and dense urban settlement. Considering the physical properties of scatters and imaging geometry, various features and suitable baseline (<300m) allow us to obtain a large range of coherence values, and the moderate relief with average elevation of 4m benefits for accurate estimation of coherence.

Table 1 Parameters of simulated deformations

Model	Group I							Group II					
	A1	B1	C1	D1	E1	F1	G1	A2	B2	C2	D2	E2	F2
subsidence (mm)	3.5	7	14	28	56	84	112	3.5	7	14	28	56	84
Fringes	1/8	1/4	1/2	1	2	3	4	1/8	1/4	1/2	1	2	3
Azimuth/Range (m)	960×480							480×320					

Deformation simulation

We consider 2-D elliptical Gaussian function as surface deformation, the correlation between two directions is set to zero in order to retrieve a "bowl" shape subsidence. For modeling purpose, the variance and peak of Gaussian function are adjusted with respect to various deformation gradients. All simulations are assumed in the range-Doppler coordinate system. In table Ⅰ, two groups of simulated deformations which represent total 13 different deformation gradients are listed. The main reasons for choosing such spatial extents are to avoid excessive image texture and to make observations as homogeneous as possible, in which accurate coherence estimation could be desired.

Observations formation

We choose 20 patches described by different coherence coefficients from initial coherence map, and also record corresponding locations of these patches at slave SLC image. An automatic threshold scheme is used to search expected value with minimum standard deviation. Then each of the simulated deformation is inserted into the resampled slave image in sequence. Moreover, each slave image together with the master image is processed by the two-pass differential approach, and the look numbers from 1 to 20 respectively are used in turn. Thus, $20 \times 13 \times 20$ samples with unique coherence coefficient, deformation gradient and the look number are obtained. Considering the influence of coherence bias on developing DDG model, all biased values are corrected with (6), (20) and (22) derived in Touzi *et al.'s* (1998).

DATA ANALYSIS AND STATISTIC

Data analysis

To determine whether the deformations are detectable in each observation, the detectability of fringes is taken into consideration. However, there have not been well-developed numerical methods for this purpose so that a visual inspection method is applied in the previous study. In this paper, we follow this criterion but consider local ML frequency estimation as an assist tool. This method is well known to be used to approximate the true local frequencies through maximizing frequency at the peak of the two-dimensional Discrete Fourier Transform (2-D DFT) (Spagnolini 1995). Nevertheless, the main withdraw of ML estimator is that the frequency of 2-D signal within the window should be constant, for non-constant case, the estimator is unreliable and residual fringe rate increase. Therefore, smaller estimate window in which the bandwidth of fringe is less and the DFT frequency oversample should be implemented to improve accuracy of estimation. Yet the algorithm can not be regard as completely automatic method in our observations since strong noise in relatively small scene (see table Ⅰ) and the presence of non-constant fringe rate increase errors of ML estimation.

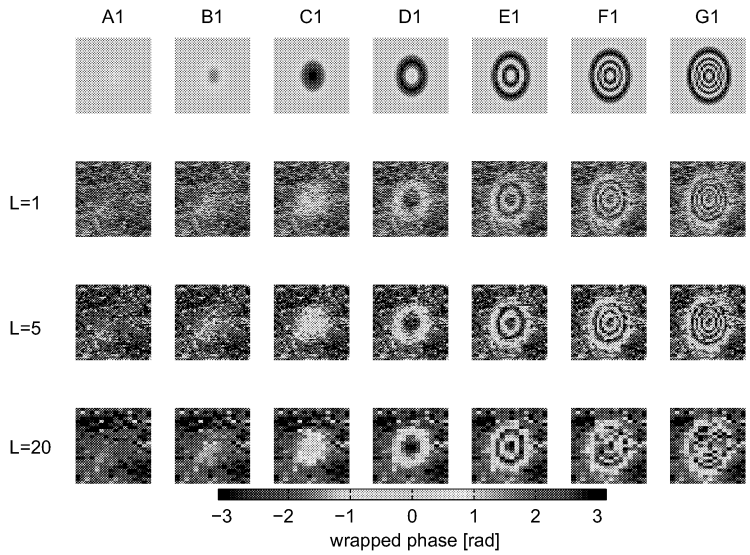

Figure 1 Observations for deformation models A1-G1 (Table Ⅰ) under L=1, 5 and 20 respectively

A group of representative observations corresponding to same coherence but different deformations and look numbers, has been shown in Figure 1. The results indicate that most of the differential interferogram patches for look numbers L=5 and 20 are clearer than those for look number L=1. However for models E1-G1 that have larger spatial gradients and denser fringes, phase aliasing can be observed in the interferogram patches with look number L=20. Comparatively, phase fringes in the interferogram patches with look number L=5 are of the best quality. For model A1, it is difficult to detect the deformation fringes under all look numbers. Therefore, it is evident that the detectability of deformation gradients in the SAR interferograms is related to the look number. Higher deformation gradients are more difficult to be detected correctly with InSAR. An appropriate look number should be chosen in multi-look operation by considering both the noise and the gradients of the expected ground deformations.

Statistic

According to observational samples and their adjustments whether or not the deformation can be successfully detected, regression analysis are carried out to determine the upper and lower bounds of the DDG as a function of the coherence values for each look number. As a demonstration, the results of statistic for the look number L=1, 5 and 20 are shown in Figure 2.

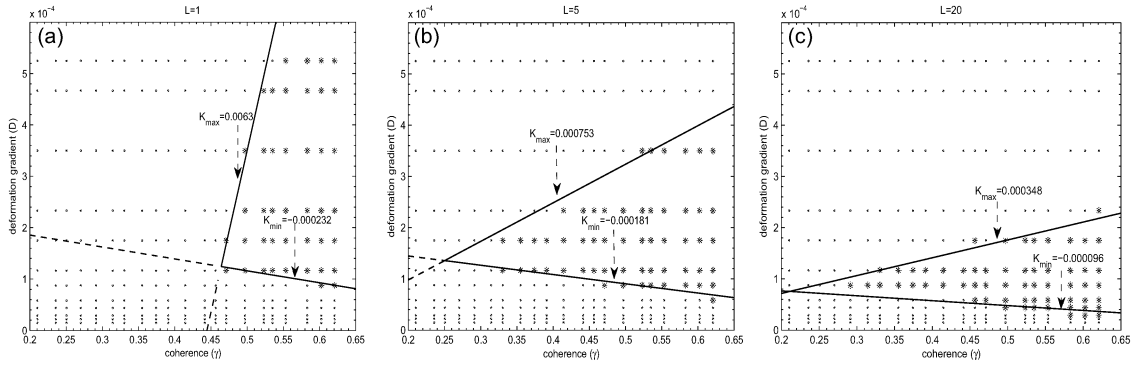

Figure 2 Observational samples and linear models of the minimum and maximum DDG for different look numbers. (a) Look number L=1. (b) Look number L=5. (c) Look number L=20. A red asterisk indicates an observational sample where the deformation gradient is detectable while a blue dot indicates the opposite.

Figure 2 shows that the minimum and maximum DDG are significantly different for various look numbers. The upper bound of the DDG becomes lower with the increase of the look number. This is due to the phase aliasing effect where the local phase slopes beyond the threshold of instantaneous frequency (phase derivative) between adjacent pixels, i.e., $|\Delta\phi| > \pi$. Multi-look operation leads to more severe phase aliasing effect. Whereas the

lower bound of the detectable DDG becomes higher with the increase of the look number as more phase noise is removed with a larger look number so that sparser phase fringes can be visible.

MODELING

Constraint

According to Baran *et al.* (2005); Massonnet and Feigl (1998), the maximum DDG under noise-free condition can reach even one fringe per pixel. Considering phase unwrapping, let us assume a sequence of phase values whose gradient is close to but slightly larger than 0.5 fringes per pixel:

$$0,\ \pi + e,\ 2\pi + 2e,\ 3\pi + 3e,\ 4\pi + 4e,\ ...$$

where e is a very small (close to zero) positive value. When it is wrapped, the sequence becomes

$$0,\ -\pi + e,\ 0 + 2e,\ -\pi + 3e,\ 0 + 4e,\ ...$$

In such a sequence, it is impossible to correctly unwrap the phases between adjacent pixels, and thus the maximum DDG should be less than 0.5 fringes per pixel. Then the definition in Massonnet and Feigl (1998) is revised into:

$$D^{0}_{\max,L} = \frac{\lambda}{4\mu_{\min,L}} \tag{1}$$

where $\mu_{\min,L}$ is the smaller pixel dimension and λ is wavelength. On the other hand, according to Massonnet and Feigl (1998), the minimum DDG under noise-free condition is 1 cm over the width of a SAR scene (100 km for ERS and Envisat data), i.e., 1×10^{-7}. Otherwise, the ground deformation mixed with such errors as the residual orbital contribution and atmospheric ramps will become undistinguishable.

Modeling

The following model is proposed to approximate the upper and lower bounds of DDG:

$$\begin{cases} D_{\min}(\gamma, L) = 10^{-7} + K_{\min}(L)\times(\gamma - 1) \\ D_{\max}(\gamma, L) = D^{0}_{\max}(L) + K_{\max}(L)\times(\gamma - 1) \end{cases} \tag{2}$$

Where $K_{\max}(L)$ and $K_{\min}(L)$ are the slopes of linear bounds under each look number and determined by linear regression. $D^{0}_{\max}(L)$ is the maximum DDG and different with various look number. It can be seen if only three unknown parameters $D^{0}_{\max}$, $K_{\max}$ and $K_{\min}$ as a function of the look number can be solved, and then the new model will be developed. Nevertheless, we can't directly deduce the relation of these parameters to the look number from regression analysis.

As $D^{0}_{\max,L}$ is the ratio between one-quarter of the radar wavelength and the smaller dimension of the multi-looked pixel $\mu_{\min,L}$, $D^{0}_{\max}(L)$ can be determined by establishing an empirical functional relationship between $\mu_{\min,L}$ and L based on the method of trial and error, which may be written as:

$$\mu(L) = \frac{4L}{ceil(\sqrt{\frac{L}{5}})} \tag{3}$$

where $ceil(x)$ gives an integer equal to or greater than x (the nearest one). Note the look number L used in (3) or interfermetric process has been decomposed along the azimuth and range directions to make the final pixel close to a "square". Furthermore, some look numbers such as L = 11, 13, 17, and 19 are removed from our study because they are insignificant for data process in practice. However, for satisfying (3) look numbers L = 6, 7, 8, 9 and 15 have to be excluded.

As stated above, no simple curve is available to represent the functional relationship between $K_{\max}$, $K_{\min}$ and L. This is too much understandable as the deformation gradient substantially rely on pixel size although multi-look operator can alter the pixel size. The relationship between $K_{\max}$, $K_{\min}$ and $\mu(L)$ is then explored, through which $K_{\min}(L)$ and $K_{\max}(L)$ can be determined.

Table 2 Slope values for different look numbers

L	1	2	3	4	5	10	12	14	16	18	20
$\mu(L)$	4	8	12	16	20	20	24	28	32	36	40
$K_{\max}(10^{-3})$	6.30	2.80	1.66	1.07	0.75	0.69	0.63	0.54	0.46	0.4	0.35
$K_{\min}(10^{-4})$	-2.32	-2.16	-2.03	-1.92	-1.81	-1.73	-1.55	-1.42	-1.27	-1.16	-1.00

Table 2 shows the regressed slope values from statistic under each look numbers. The scatter plot of $\mu(L)$ versus $K_{\max}$ and $K_{\min}$ is shown in Figure 3. It is clear that with the increase of $\mu(L)$, $K_{\max}$ decreases monotonically and $K_{\min}$ increases linearly. Therefore, the power equation and linear function can be respectively used to approximate them. We adopt linear least squares fitting method to solve the coefficients of both equations, and the results are also shown in Figure 3. To avoid ill-conditioning in the coefficient matrix, the two values at $\mu(L)$=20 (when $L = 5$ and 10) are merged into one by taking their mean value in the regression. For $K_{\max}(L)$ the RMSE value between the observed and the fitted values is 7.388×10^{-5}, and the confidence bounds for fitted coefficients under 95% confidence levels are $(0.0333, 0.0393)$ and $(-1.306, -1.210)$ respectively. Similarly, the RMSE value of function $K_{\min}(L)$ is up to 2.69×10^{-6}, and confidence bounds for coefficients are $(3.525\times10^{-6}, 3.867\times10^{-6})$ and $(-2.515\times10^{-4}, -2.430\times10^{-4})$. It should be pointed out that high-order polynomial may be more accurate for fitting $K_{\max}$ than that of power equation. However, when $K_{\max}$ is extrapolated for larger look number, e.g., an optimal multi-look factor for glacier motion monitoring (Hoen and Zebker 2000), the fitted value diverges significantly, and therefore the model can't be used to predict detectable deformation.

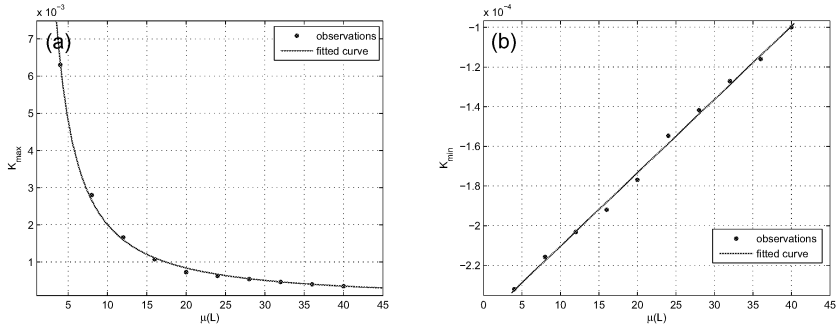

Figure 3 Plot of $\mu(L)$ versus $K_{\max}$ (a) and $K_{\min}$ (b) respectively as well as the best-fit lines

Finally, combining (1)-(3), regression models $K_{\min}(L)$ and $K_{\max}(L)$, a general functional model for the minimum and maximum DDG for Envisat ASAR/ERS interferometry can be obtained:

$$\begin{cases} D_{\min}(\gamma, L) = 10^{-7} + \left(0.000003696\times\mu(L) - 0.0002473\right)\times(\gamma - 1) \\ D_{\max}(\gamma, L) = \dfrac{\lambda}{4\mu(L)} + \left(0.03632\times\mu(L)^{-1.258}\right)\times(\gamma - 1) \end{cases} \tag{4}$$

RESULTS

An Envisat ASAR pair acquired on 13 November 2007 and 01 April 2008 over Zhengzhou, Henan Province, China, is used to validate the new model. The perpendicular baseline is approximately 30 m. we process the pair with GAMMA software and three differential interferograms are produced respectively under the look number $L = 1,\ 5$ and 20. A representative ground subsidence is then extracted and shown in Figure 4, which is to verify whether the new model is able to correctly predict the detectability of deformation under different look numbers.

To perform the validation, two model parameters should be estimated. The mean value of coherence over the rectangular area is 0.36, which has been corrected by unbiased algorithm. The fringe rate along OC direction (see Figure 4(a)), are determined by local ML frequency estimation. We estimate the fringe signal over the rectangular area with 2-D DFT, and interpolate DFT by a factor 32 to better detect the exact fringe numbers. From the Figure 4(b) it can be seen the locations of peaks (red points) along OC direction are different under each look number. Only the fringe number when $L = 5$ is basically identical with the result of visual inspection. Then the deformation gradient between points O and C are approximated to be 0.14×10^{-3} (2 fringes over a distance of 400m). Finally, substituting both parameters into (4), optimal multilook operator to detect deformation can be obtained. For the sake of simpler and more intuitive notation, graphic expression of (4) is shown in Figure 5. We plot the result into it and the point $(0.36, 0.14 \times 10^{-3})$ falls into the region where the deformation gradient can only be detected when $L = 5$. The case agrees well with the reality.

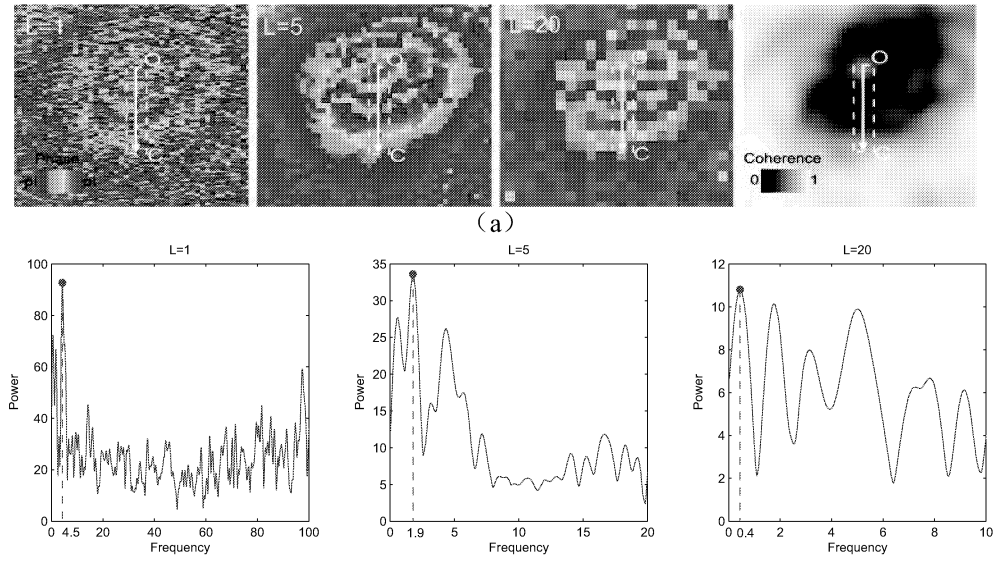

Figure 4 (a) Differential interferograms ($L = 1,\ 5$ and 20) and corresponding coherence map; (b) Local frequency estimation along OC direction

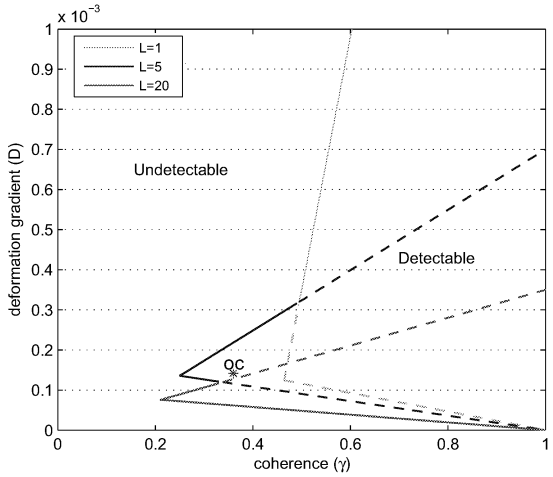

Figure 5 Results of model validation

CONCLUSIONS

A general model for determining the minimum and maximum DDG has been established. The model incorporates both the interferometric coherence and the look number, representing an extension to the previous work that only considers the coherence. The new model considered useful in assessing the ability of InSAR in

detecting ground deformations and in providing guidance in choosing appropriate look numbers in InSAR data processing.

ACKNOWLEDGMENTS

This work was supported by the National Natural Science Foundation of China (Nos. 40974006 and 40774003), a High-Tech Research and Development "863" Program of China (No. 2006AA12Z156), the Research Grants Council of the Hong Kong Special Administrative Region (Nos.: PolyU5161/06E and PolyU5155/07E), and Key Laboratory of Geo-informatics of State Bureau of Surveying and Mapping. The Envisat data used in this study were provided by the European Space Agency under Category 1 projects (AO-4458 and AO-4914).

REFERENCES

Ding, X.L., Liu, G.X., Li, Z.W., Li, Z.L. and Chen, Y.Q. (2004). "Ground subsidence monitoring in Hong Kong with satellite SAR interferometry", *Photogrammetric Engineering and Remote Sensing*, 70(10), 1151-1156.

Wang, T., Liao, M.S. and Perissin, D. (2010). "InSAR coherence-decomposition analysis", *IEEE Geosci. Remote Sens. Lett.*, 7(1), 156-160.

Li, Z.W., Ding, X.L., Huang, C. and Zou, Z.R. (2007). "Atmospheric effects on repeat-pass InSAR measurements over Shanghai region", *J. Atmos. Sol-Terr Phy.*, 69, 1344-1356.

Baran, I., Stewart, M. and Claessens, S. (2005). "A new functional model for determining minimum and maximum detectable deformation gradient resolved by satellite radar interferometry", *IEEE Trans. Geosci. Remote Sens.*, 43(4), 675-682.

Massonnet, D. and Feigl, K. (1998). "Radar interferometry and its application to changes in the Earth's surface", *Review of Geophysics*, 36(4), 441-500.

Bamler, R. and Hartl, P. (1998). "Synthetic aperture radar interferometry", *Inv. Prob.*, 14(4), R1-R54.

Touzi, R., Lopes, A., Bruniquel, J. and Vachon, P.W. (1999). "Coherence estimation for SAR imagery", *IEEE Trans. Geosci. Remote Sens.*, 37(1), 135-149.

Spagnolini, U. (1995). "2-D phase unwrapping and instantaneous frequency estimation", *IEEE Trans. Geosci. Remote Sens.*, 33(3), 579-589.

Hoen, E.W. and Zebker, H.A. (2000). "Penetration depths inferred from interferometric volume decorrelation observed over the Greenland ice sheet", *IEEE Trans. Geosci. Remote Sens.*, 39(2), 2571-2583.